



# Resilience enhancement program in smart grids by coordinating demand response and optimal reconfiguration during wildfires

Sasan Najibi<sup>1</sup> · Mojtaba Najafi<sup>1</sup> · Mehrdad Mallaki<sup>1</sup> · Najmeh Cheraghi Shirazi<sup>1</sup>

Received: 25 April 2023 / Accepted: 13 September 2024

© The Author(s), under exclusive licence to Springer-Verlag GmbH Germany, part of Springer Nature 2024

## Abstract

Power grids have experienced significant damage and disruption due to wildfires. The spread of wildfires affects the electricity grid by reducing the transmission capacity of overhead lines while decreasing the efficiency of power plants. When wildfires spread, the main challenges are to change the network configuration and manage power consumption to improve network resilience. Network reconfiguration is accomplished by switching transmission lines and changing the network topology. Energy consumption management is also conducted using demand response (DR) methods. However, load prioritization has received less attention in DR methods. The purpose of this paper is to improve the resilience of the power grid against wildfires by introducing a framework for grid recovery and providing power for high-priority loads. For this purpose, a novel multi-objective optimization problem is proposed, which considers optimal topology and DR programs, and aims to maximize the restored critical loads and network flexibility. In the proposed framework, the spread of fire is also considered in a probabilistic form. The effectiveness of the proposed method is confirmed by simulating on the 33-bus test systems.

**Keywords** Power grid resilience · Wildfire · Demand response · Grid reconfiguration

## List of symbols

### Parameters

$P_{G,i,\ell}$	Power plant capacity at bus $\ell$
$i; p; q$	Indices of nodes in the distribution system
$S_\ell^{\min}$	Minimum battery SOC allowed at bus $\ell$
$d$	Index of DR blocks
$S_\ell^{\max}$	Maximum battery SOC allowed at bus $\ell$
$L$	Set of nodes with loads
$R_{q-l}$	Reachability between the node $q$ and $\ell$
$N$	Set of all nodes in the post-disaster distribution system
$R_{dbat,\ell,i}$	Ramp-down service of the battery at bus $\ell$ at a time $i$

$G$	Set of nodes with distributed generations
$R_{ubat,\ell,i}$	Ramp-up service of the battery at bus $\ell$ at a time $i$
$E$	Set of all available lines in the post-disaster power grid
$\frac{B_{bat}^\ell}{P_q}$	Power capacity of the battery at bus $\ell$
$\bar{B}_{bat-en}^\ell$	Average power demand at load point $q$ after DRP
$\Psi$	The energy capacity of the battery storage at bus $\ell$
	Set of nodes of the loads with DR programs

### Variables

$\Upsilon$	Set of DR blocks of the load $i$
$P_i^D$	Power reduced by DR program at node $i$
$\Gamma_i$	Priority factor of the load at node $i$
$I_{ij}$	Flowing current of the line $(i; j)$
$\Phi_i$	Priority factor of DR block $d$ of the load $i$

✉ Mojtaba Najafi  
mojtabanajafi2000@gmail.com; mojtaba.najafi@iau.ac.ir

<sup>1</sup> Department of Electrical Engineering, Bushehr Branch, Islamic Azad University, Bushehr, Iran

$P_{ij}/Q_{ij}$	Active/reactive power flow of the line (i; j)
$y_s$	Probability of cell start to burn
$P_i^{In}/Q_i^{In}$	Injected active/reactive power at node i
$P_{id}^{StepDR}$	Capacity of DR block d of the load i
$P_i^G/Q_i^G$	Generated active/reactive power at node i
$V_i^{\min}/V_i^{\max}$	Upper/lower limit of voltage magnitudes
$V_i$	Voltage magnitude at node i
$P_i^B/Q_i^B$	Total target active/reactive power demand in the system normal operating state
$P_i^L/Q_i^L$	Restored active/reactive load at node i
$X_{ij}/R_{ij}$	Resistance/reactance of the line (i; j)
$w_i$	Binary variable representing status of the load i after optimization
$P_i^{DG, \min}/Q_i^{DG, \min}$	Lower limit of reactive power of DGi
$c_{id}$	Binary variable representing status of DR block d of the load i
$P_i^{DG, \max}/Q_i^{DG, \max}$	Upper limit of reactive power of DGi
$\zeta_{ij}$	Binary variable representing status of the switch between bus i and bus j
T	Total time duration
Te	Long the battery power and the PV generation can last
$S_{\ell, i, j}$	Energy remained in the battery at bus $\ell$ for a time i in scenario j
$p_{bat\_cha, \ell, i, j}$	Charging power for an hour i at bus $\ell$ in scenario j
$\eta^+$	Battery charging efficiency
$p_{bat\_dis, \ell, i, j}$	Discharging power of for an hour i and at bus $\ell$ in scenario j
$\eta^-$	Battery discharging efficiency
$\psi_{bat\_cha, \ell, i, j}$	Status variables indicating whether the battery on bus $\ell$ is charging at a time i in scenario j
$S_{i, j}^0$	The initial state of charge (SOC) of the battery
$\psi_{bat\_dis, \ell, i, j}$	Status variables indicating whether the battery on bus $\ell$ is discharging at a time i in scenario j

## 1 Introduction

Due to global warming and human activities, the number and intensity of wildfires are expanding worldwide. Wildfires may get out of control and approach residential as well as industrial areas, affecting the power transmission

lines and plants. The increased heat caused by the fire may reduce the power transmission capacities of overhead transmission lines. Recently, power grids have sustained significant damage and disruption due to wildfires [1]. Wildfires can negatively affect electricity generation, transmission, and distribution. According to [2], wildfires have destructive effects on the power grid. For instance, the capacity of photovoltaic cells is changed under the influence of heat transfer, soot, and smoke. Moreover, physical damage to overhead transmission lines, poles, transformers, and substations affects the performance of the power grid. In addition, the increase in ambient temperature also reduces the capacity of transmission lines [3].

In the last decade, wildfires have damaged power grids in different countries. As mentioned in [4], the 2017 Thomas fire interrupted transmission lines in the Santa Barbara area, leaving more than 85,000 customers without electricity. In 2018, about 50,000 customers lost their electricity while the Mendocino Complex continued to burn down neighborhoods in Mendocino County.

In recent years, the power grid resilience problem has attracted much attention from companies and researchers. Power grid resilience means the ability of the grid to withstand and recover from deliberate or naturally occurring threats or incidents [5]. One of the main challenges in defining the resilience of a power grid is to suggest an appropriate measurement metric that clearly reflects the defined concept of resilience. The resilience measure should be useful for decision making, comparable, and quantitative [6]. In other words, as wildfires increasingly threaten power grids due to global warming and human activities, there is a critical need to enhance grid resilience. While past research has examined grid resilience against various natural disasters, specific studies on wildfire impacts are limited. Existing approaches often lack integration of demand response programs (DRPs) and optimal grid reconfiguration strategies.

In previous researches, power grid resilience was investigated from different perspectives. Although the results of those works can be used to improve grid resilience against some events such as floods, earthquakes, and hurricanes, for various reasons, grid resilience enhancement for wildfire should be studied separately. The first important reason is that different extreme events have different impacts on power grid. For instance, as mentioned in [7], power demand variations may be different during various extreme events. Also, impacts of the events may be different to each other. Some impacts of different events are summarized:

1. Transmission lines are affected by high temperatures and heat waves, resulting in limited transfer capability and increased energy losses. Additionally, these conditions can cause the lines to sag.

2. Storms and hurricanes with high winds can cause faults and damage to overhead transmission and distribution lines. This can occur when debris is blown against the lines or in extreme cases, when a tower collapses due to the strong winds.
3. Failures of overhead lines and towers can also be caused by cold waves, heavy snow, and the accumulation of ice. In freezing conditions, ice and snow can gather on insulators, creating a conducting path that leads to flashover faults.
4. Short-circuit faults can be triggered by lightning strikes on or near overhead conductors. This results in the activation of electrical protection systems and the disconnection of the lines. Although these faults are usually transient and quickly restored, the voltage surge from the strike can cause damage to equipment such as transformer wings.
5. While rain and floods do not pose a direct danger to overhead transmission lines, they can be a threat to substation equipment such as switchgear and control cubicles. The combination of rain with strong winds or lightning, however, can pose a significant risk to overhead lines.
6. Flood and earthquake can damage to substations, power generators, and transmission towers [7].

In addition, events intensity and impacts of them may be different with each other. Grid recovery time is dependent to different factors such as grid infrastructure and event intensity. However, during the most disasters such as floods and earthquakes, electricity equipment might be destroyed or not, and the undamaged equipment usually can continue to operate normally. While, in wildfire in addition to that some equipment is completely damaged or taken out of service, the performance of some undamaged equipment may be decreased due to a rise in environmental temperature and soot [8].

Power grid performance against wildfire has been studied in some research papers. For instance, authors [9] presented a practical decision support approach that combines a stochastic wildfire simulation method with an attacker-defender model. The objective was to identify the worst-case scenario for transmission line and generator contingencies, as well as wind and solar power trajectories. The approach utilized a max-min structure, where the inner min problem represents the optimal adaptive response for generator dispatch actions. Additionally, the paper introduced an evaluation framework to assess the power supply security of different power system topology configurations. This assessment was conducted under the assumption of limited transmission switching capabilities and involved simulating multiple wildfire evolution scenarios. The modeling framework presented in [10] encompassed several components. Firstly, clustering algorithms were utilized to identify communities using

building footprint data, fire hazard severity, and renewable energy potential. Secondly, a building simulation model was employed to quantify the energy demand. Lastly, an energy system optimization model was utilized to aid in the design of the microgrid. Additionally, a novel optimization tool was introduced to effectively model microgrids in the wild land-urban interface.

The spread of wildfires among system components adds further complexity to the problem, making it mathematically challenging and requiring complex modeling. Operators must make quick decisions during sequential failures to ensure reliable operation and prevent cascading failures and blackouts. This complexity is further amplified during extreme weather events. Hence, researchers in [11] proposed a proactive generation dispatch strategy that used probabilistic methods to enhance the operational resilience of power grids during wildfires. A Markov decision process was employed to model system state transitions and provided generation dispatch strategies based on component failure probabilities, wildfire characteristics, and load variations.

The research that was presented in [12] introduced a novel approach to address the issue of wildfires and their impact on distribution grids. The proposed strategy focused on proactive actions that aimed to enhance the operational resilience of these grids. The paper began by modeling the effects of wildfires on power distribution systems. This was achieved by mathematically formulating the impact of the wildfire and the heat; it generates on the capacity and status of power lines. The paper also took into account the effects of wildfire byproducts such as heat, smoke, and ash on renewable power generation, specifically solar and wind energy. Furthermore, a stochastic optimization problem was developed to incorporate the various impacts of wildfires on the system, while considering physical, operational, and environmental constraints. To ensure a comprehensive approach, an objective function was introduced that takes into consideration both grid resilience and equity criteria during system contingencies. Suggested approach in [13] was centered on minimizing the disruptions caused by wildfires, which have the potential to pose risks to both electrical equipment and the safety of personnel. To achieve this, that framework began by providing a comprehensive package for characterizing wildfires. That package enabled the monitoring and analysis of various aspects of wildfires, such as their intensity, arrival time, and the paths, they take from ignition points to electrical equipment. Additionally, authors proposed a decision support tool specifically designed for managing wildfires in power grids. That tool allowed for the effective utilization of local generation resources, including distributed renewable energy resources and energy storage systems, to mitigate the impacts of wildfires on the power grid.

The performance of the power grid can be evaluated using various criteria. For example, reference [14] presents

**Table 1** Research literature

References	Main Contribute
[9]	Diagnosis the worst case for the distribution grid and generators during wildfire based on min max method
[10]	Develop microgrid based on renewable distributed generations (DG)
[11]	Increased the power grid resilience during wildfire based on Markov model and generation dispatch strategies based on component failure probabilities
[12]	Focus on proactive actions during wildfire to increase resilience power grid. The paper also took into account the effects of wildfire byproducts such as heat, smoke, and ash on renewable power generation, specifically solar and wind energy
[13]	Minimize the disruptions caused by wildfires. authors proposed a decision support tool specifically designed for managing wildfires in power grids
[14]	Presents a two-stage stochastic framework for scheduling resources in microgrids, examining the impact of flexible loads on the power grid
[15]	Use microgrid to enhance power grid reliability
[16]	robust forecasting methods for short-, medium-, and long-term loads
[17]	Focus performance of power plants by proposing a multi-objective solution to balance production and demand

a two-stage stochastic framework for scheduling resources in microgrids, examining the impact of flexible loads on the power grid. According to [15], microgrids can enhance power grid reliability, and the research proposes an optimized method for microgrids that combines solar and green energy sources. To develop an effective demand response program, it is crucial to have robust forecasting methods for short-, medium-, and long-term loads, as highlighted in [16]. While much research focuses on the performance of the distribution network, the performance of power plants should also be considered. Reference [17] addresses this issue by proposing a multi-objective solution to balance production and demand. Table 1 shows the research literature.

Our studies reveal two significant research gaps in power grid resilience study during wildfires. First, while grid resilience has been investigated under various conditions, the resilience of distribution grids during wildfires has received less attention from researchers. There is a need for the development of new optimization problems in this scope. Second, there is a notable gap in the optimal configuration of power distribution grids during wildfires, particularly with respect to the spread probability of the wildfire. Hence, in

this research, a novel method is developed to improve network resilience during a wildfire. The proposed framework aims to calculate power grid parameters and reconfiguration of the power grid during wildfires. The utilization of demand response program (DRP) enhances the efficiency of the power grid and effectively manages power demand [18]. Therefore, this research takes a unique approach by considering DRP. It is important to note that within the power grid, different loads possess varying levels of priority and significance, and not all loads may participate in the DRP. Consequently, the proposed framework takes into account both load priority and DRP. One notable advantage of this framework is its incorporation of storage devices within the power grid. Then, the multi-objective problem is defined to calculate optimal topology and variables of the power grid. This problem also considers the probability of wildfire spreading, where areas located farther from the wildfire are deemed more valuable than those in close proximity. Hence, the regions with a higher likelihood of wildfire are assigned a lower weights, which this weights determined by the probability of fire in those specific areas. This assumption is based on the understanding that electrical equipment near wildfire areas is more susceptible to damage or being deactivated by protective systems. The multi-objective problem incorporates three metrics. The first objective function aims to maximize the flexibility of the power grid, enabling it to recover to normal conditions. The second metric, capacity accessibility, strives to provide the maximum electricity capacity for the power grid during a wildfire. Additionally, the third function is defined to prioritize power supply for loads with higher priorities. Ultimately, the resilience of the power grid is evaluated using various indices, including power grid flexibility, capacity accessibility, EDNS, and LOLP.

Overall, this research provides a novel approach to enhancing power grid resilience during wildfires by integrating advanced optimization techniques, load prioritization, and probabilistic fire spread considerations, thus addressing key gaps in the current literature. This paper makes several significant contributions to the power grid resilience, specifically in the context of wildfires:

- Novel framework for grid resilience: The paper introduces a comprehensive framework designed to enhance the resilience of power grids during wildfires. This framework integrates two key components: (i) an optimized network reconfiguration strategy and (ii) an advanced demand response (DR) program. The framework addresses the unique challenges posed by wildfires by focusing on dynamic grid reconfiguration and effective load management.
- Development of multi-Objective optimization problem: A novel multi-objective optimization problem is proposed

to improve grid resilience. This problem simultaneously considers optimal network topology and demand response programs, aiming to maximize the restoration of critical loads and network flexibility. Importantly, the optimization problem incorporates the probabilistic spread of wildfires, allowing for a more realistic and adaptive approach to managing the power grid under wildfire threats.

- Integration of load prioritization in demand response: The paper highlights the underexplored aspect of load prioritization within demand response methods. By incorporating load prioritization, the proposed framework ensures that high-priority loads receive power even during severe wildfire events, thereby enhancing overall grid reliability and operational efficiency.
- Consideration of fire spread probability: Unlike previous research, this framework integrates the probability of wildfire spread into the optimization process. This probabilistic approach allows for better anticipation and management of wildfire impacts, leading to more effective and resilient grid operation strategies in the face of fire threats.

The graphical abstract is shown in Fig. 1. Also, the rest of the paper is organized as follows: In Sect. 2, the effect of wildfires on the power grid is investigated. The proposed framework and model assumptions are introduced in Sect. 3. In Sect. 4, the mathematical problem formulation is described. Numerical simulation results are reported in Sect. 5; and finally, conclusions are presented in Sect. 6.

## 2 Wildfire effect on power GRIDS

### 2.1 Transmission lines

A wildfire is an unintentional natural or deliberate-caused fire occurring in a natural setting. It affects power grid components that are exposed to it. The damages can occur either through direct contact such as a fire in generators and substations or indirectly by increasing the temperatures beyond the maximum levels for equipment and transmission lines. Overhead line capacities are sensitive to wildfires. Excess heat released due to the wildfire can increase the surface temperature of the conductor. Moreover, temporary sagging of the conductors decreases their distance from the ground and increases the probability of flashover. Overhead line conductors have a maximum operating temperature that should not be surpassed. This maximum temperature determines the rating of the line. Although heat transfer from a wildfire through convection is possible in some cases, heat is often transferred through radiation. Consequently, the convective heat transfer due to wildfires has been ignored in this study. Due to the fire, the capacity of transmission lines may be reduced. The maximum capacity of transmission lines is obtained as

follows [19]:

$$I^{\max} = \sqrt{\frac{Q_c + Q_r - Q_s - Q_{rf}}{R_c(T_{c,\max})}} \quad (1)$$

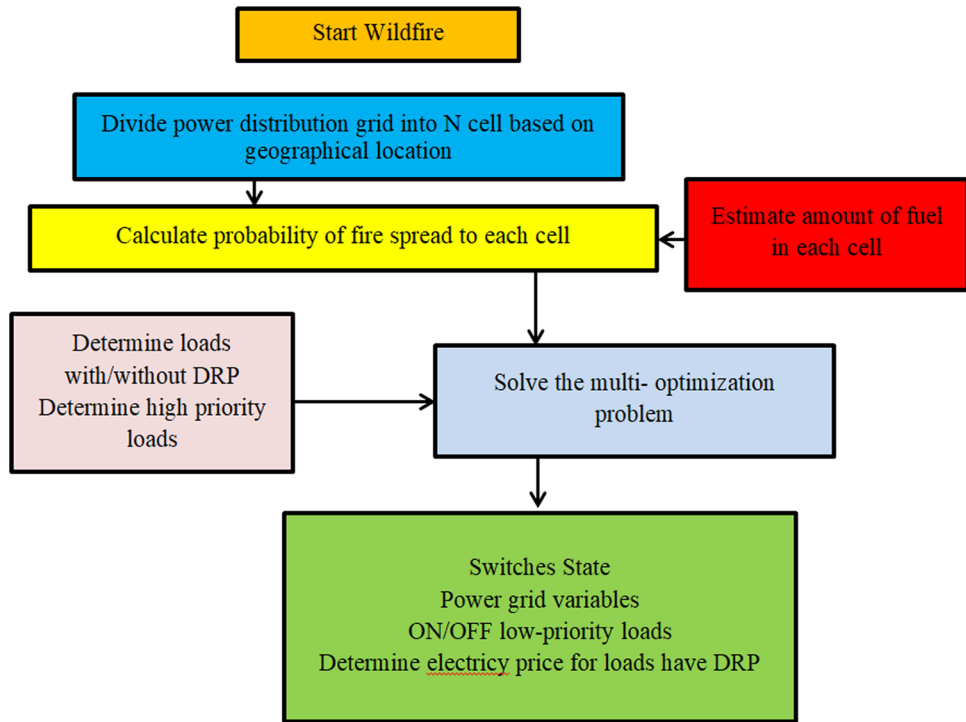
where  $Q_c$ ,  $Q_r$ ,  $Q_{rf}$ , and  $Q_s$  are the convective heat loss rate per unit length of the conductor, the radiative heat loss rate per unit length of the conductor, the radiative heat gain rate per unit length of the conductor, and the solar radiant heat gain rate per unit length of the conductor, respectively. These parameters are related to flame length, flame width, tilt angle, rate of spread, distance between transmission line, height above the ground, and flame zone wind speed, and their details are presented in [20].

### 2.2 Power plants

The efficiency of thermal power plants decreases under the influence of heat. The increase in heat caused by the fire leads to the reduction of the thermal efficiency of the thermal power plant. Thermal power generations use different cooling technologies. Two crucial technologies are once-through cooling (OTC) and closed-loop cooling (CLC) systems. OTC systems require a large volume of water. In the CLC technology, water is circulated in the cooling loop, including a cooling tower, where a small portion of cooling water evaporates. The CLC technology is considered in this research. For CLC technology, the effect of the air temperature on the power capacity can be modeled based on [21].

Renewable energy sources like solar photovoltaic are being increasingly utilized to meet electricity demands in a sustainable manner. However, the performance of solar photovoltaic can be hindered by extreme events such as wildfires and the resulting widespread smoke. It can be challenging to isolate the specific impact of smoke on photovoltaic energy production and separate from other ambient conditions. While the direct damage caused by wildfires is a significant concern due to the extensive destruction it causes, there are also secondary effects in the form of smoke. The smoke contains fine particulate matter that reduces air quality and visibility. Moreover, wildfire smoke often covers a much larger area than the actual burn area of the fire itself. This has adverse consequences for solar photovoltaic (PV) energy production, adding further stress to the power grid. The heavy smoke limits the amount of solar radiation that can reach the solar collection panels, and understanding the extent of the impact on energy production can aid in grid planning and operational decision making.

The propagation of smoke from wildfires is influenced by factors such as wind speed, wind direction, terrain, and most importantly, the burn patterns of the fires. Extensive research has been conducted to improve the forecasting of wildfire smoke severity and transport, which can help provide

**Fig. 1** Graphical abstract

advance warning of the impact on solar energy production. However, the understanding of how smoke specifically affects solar PV production is still limited [22].

### 3 Proposed framework

The proposed framework introduced in this paper has three main purposes. The first aim is to determine optimal topology for the power grid during or after a wildfire, and the second one is to provide electricity for high-priority loads during or after a wildfire. The third purpose is to calculate variable setting of the power grid during wildfires. It is assumed that the distribution network has several power plants, transmission lines, and loads that are scattered in a geographical area. Several DGs are also used to generate power. Storage devices are used to store energy in some hours and inject energy into the grid in other hours. The power grid contains transformers to change voltage level or to isolate powered devices from the power source. Usually, transformers are located near DGs or buses. Performance of transformers can be modeled with the corresponding bus or DG. For a particular bus, if the bus has been damaged or taken out of service by wildfire, then it is likely that the transformer connected to it has also been damaged by the wildfire or taken out of service by its protection systems and vice versa.

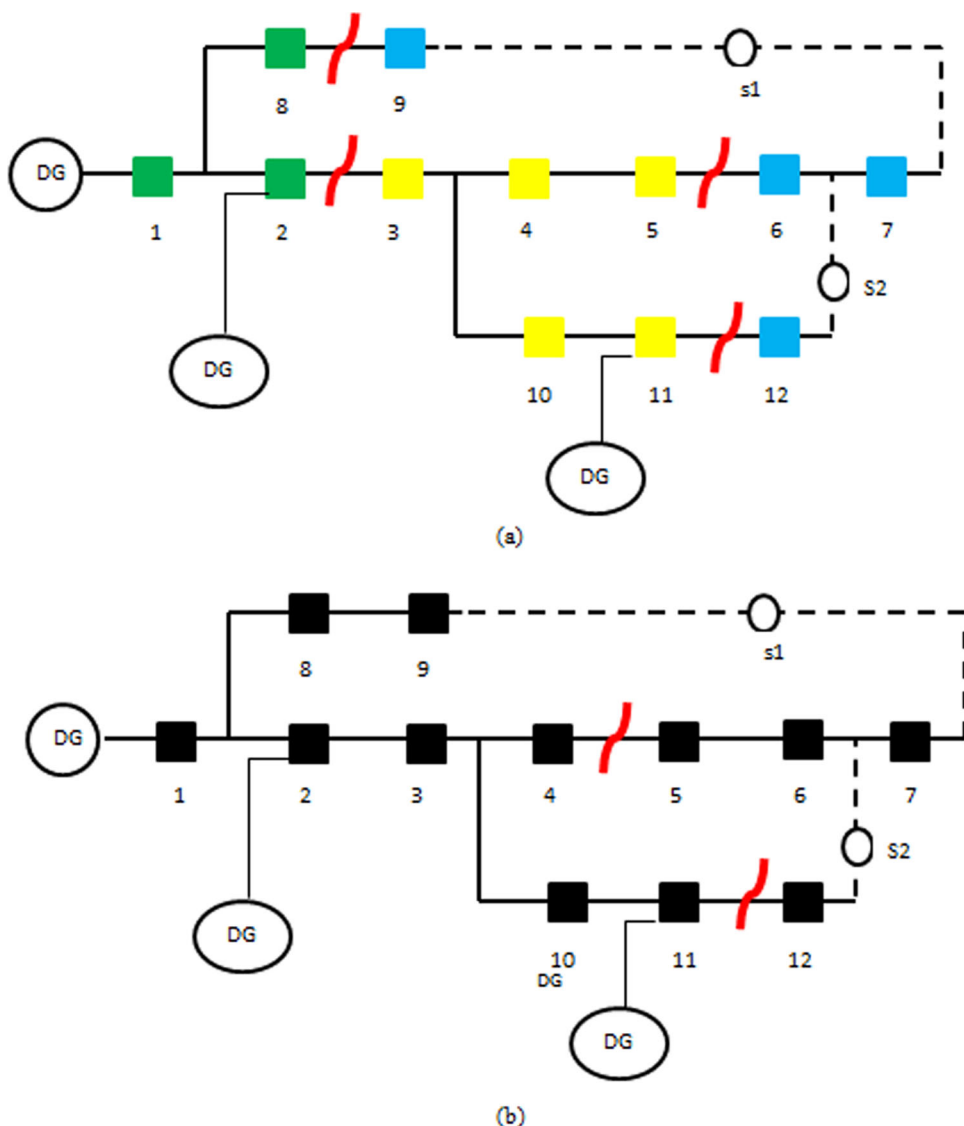
During a wildfire, some DGs and transmission lines may be damaged. Damaged lines can be replaced with alternative ones, and this causes the network topology to change. It

is possible to change the network topology using switches. There are several maneuvering switches in the network that will be closed after a wildfire. The purpose of these switches is to supply loads from alternative routes. In this paper, it is assumed that after a wildfire, some substations are in outage mode, and the main grid cannot supply the distribution network anymore. Due to the loss of transmission lines and some equipment, the distribution system could rely just on local DGs. Therefore, several electrical islands can be formed. By further interconnecting these islands via closing possibly survived tie lines and switches, larger islands with more local resources can be created. Once the switches are closed, the network may be in several different configurations, as shown in Fig. 2:

1-Some loads may be interrupted, and it is not possible to supply them. In Fig. 2a, it is assumed that transmission lines between buses 5–6, 8–9, and 11–12 are disconnected due to wildfires. It can be seen that after closing the switches, some loads (are shown in blue) are disconnected from the network. Therefore, there is no power supply for these loads, and parts of the network may be completely without electricity in case of wildfire. A solution to overcome this problem is the optimal placement of DGs, storage devices, and switches, which is outside the scope of this research.

2-As shown in Fig. 2a, it is possible that after connecting the switches, the network is divided into several separate islands. In this case, each island contains several loads, storage devices, and DGs. These islands are not electrically connected, and they cannot exchange energy with each other.

**Fig. 2** Reconfiguration of power grid after wildfires



However, it is necessary to optimize the performance of all these islanded sub-grids, separately. In this figure, it is observed that green buses and yellow buses are disconnected to each other and operated as island microgrids.

3-Fig. 2b indicates that, when the switches are closed, all loads, storage devices, and DGs connect to the power grid. In this figure, tie lines and switches provide power for buses 5–7 and 12.

However, the proposed framework has some limitations. Although we consider storage devices in this research, the optimal scheduling for charging and discharging of storage devices does not consider in this framework. In fact, for optimal use of storage devices, we need to define a new objective function to schedule the charging and discharging of storage devices.

The probability of spreading fire in the environment may depend on several factors such as speed and direction of

wind and so on. The behavior of wildfires is a complex and ever-changing phenomenon. Various factors such as fuel availability, weather conditions, wind speeds, and topography play a crucial role in determining the spread of a wildfire. These characteristics not only dictate the time and area at risk of burning but also influence the potential impact on the power system. The scientific literature offers two types of models to describe fire dynamics. The first type relies on probabilistic or statistical models, while the second type utilizes computational fluid mechanics or similar approaches. In this study, we adopt a mathematical model based on a probabilistic framework, as outlined in [9]. To simulate the area of interest, we divide it into a grid of square cells, each characterized by an initial fuel level, geographical boundaries, and a parameter that governs the rate at which fire spreads to neighboring cells. Our simulation model employs the following notation: the cells within the defined area  $S$  are denoted

by  $i$  or  $j$ , and time is represented by  $t$ . Additionally, we use the binary state  $x$  to indicate whether a cell is burning (1) or not (0) during a specific period.

The variable  $F$  corresponds to the amount of fuel present in  $i$ th cell at time  $t$ . The parameter  $F$  represents the fuel threshold required for a cell to ignite. The intensity of fuel consumed by  $i$ th cell during period  $t$  is denoted by  $I$ . Finally, the initial intensity of a burning cell is denoted as  $I_{i,0}$ . Based on this notation, the stochastic nature of fire dynamics can be expressed using following equations, which represent the probability of fire propagation from  $i$ th cell to  $j$ th cell. In order to model the wildfire effects on the grid, the geographical location is divided into  $S$  areas. Each area contains several power plants or loads. Fire can spread from one area to another. The spread of fire depends on several factors. The probability of a fire starting in each area at the moment  $t$  is obtained from the following equation [9]:

$$y_s = \begin{cases} 1 - \prod_{i \in Z_j} (1 - \rho_{(i,j)} \cdot x_{it}), & F_{jt} > F_{tr} \\ 0, & F_{jt} \leq F_{tr} \end{cases} \quad (2)$$

where  $y_s$  shows area  $s$  starts to burn at time  $t$  due to fire in its neighbor cells, and:

$$\rho_{(i,j)} = 1 - \exp(-\delta(i,j) \cdot \Delta t) \quad (3)$$

where  $F_{jt}$  is the amount of fuel in the cell  $j$  in period  $t$ , and  $F_{tr}$  is the threshold fuel for a cell to burn. Parameter  $\delta(i,j)$  determines the likelihood of fire spreading from the  $i$ th cell to the  $j$ th cell. In addition,  $x$  is a binary state for the fire condition and is equal to 1 if the cell is burning in period  $t$ . The parameters employed above can be estimated by various methods such as [18].

The fire spread coefficients,  $\delta(i,j)$ , and the initial fuel quantity in each cell are the crucial factors. In this scenario, when an ignition point is initially set, the model assesses the fire spread in neighboring cells that have enough fuel and extends it with probability  $y_s$ . The fuel quantity decreases as the cell fire intensity increases, which can be influenced by the intensity of neighboring cells, determined by the propagation probability between them. The following algorithm describes the proposed model for simulation probability of wildfire spread:

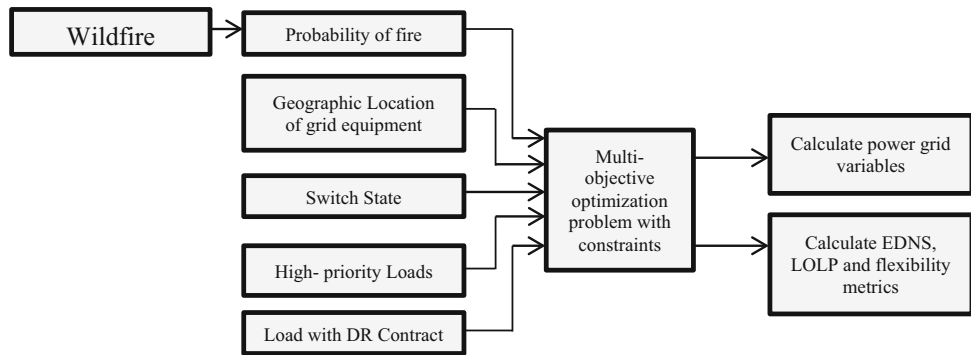
```

Initial fire focus →  $x_{i,0} = 1$ 
for  $t \in T$ , for  $i \in S$  do
    if  $x_{it} = 0 \& F_{it} \geq F$  then
        for probability  $y_s$ , do
             $x_{it} = 1 \& I_{it} = I_{i,0}$ 
             $F_{it} = F_{i,(t-1)} - I_{it}$ 
        end do
    else if  $x_{it} = 1 \& F_{it} \geq F$  then
         $x_{it} = 1 \& F_{it} = F_{i,(t-1)} - I_{it}$ 
         $I_{it} = I_{i,(t-1)} + \sum_{j \in N_i} I_{j(t-1)} (1 - \rho_{(i,j)}(x_{j,t}))$ 
    else
         $x_{it} = 0 \& I_{it} = 0$ 
    end if
end for

```

There are several models for investigating power grid resilience. In this research, the model introduced in [19] is used, where the resilience metric is employed for quantifying the resilience level of a power system during an event. The resilience of the power grid is decreased during a wildfire. This model includes three important phases including the disturbance, post-disturbance, and the recovery phase. During the disturbance phase or a disaster phase, the resilience level drops from normal resilience to post-disturbance resilience. In the post-disturbance or post-disaster phase, the system resides at the post-disturbance degraded operational and infrastructural state. The duration of this period may be varied for different wildfires. The wildfire disturbance phase may continue for several days, which is one of the important differences between a wildfire and other severe natural events. In the post-disturbance phase, the power grid is in the worst possible condition. The most crucial difference between this phase and the previous phases is the stability of the grid topology. In this phase, some harmful effects of wildfires, such as heat and soot, may disappear quickly. The capacity of the remaining parts of the network will quickly return to normal, but the complete recovery of the network due to some adverse impacts may take several days. The proposed framework can be used for both phases.

As previously mentioned, various loads are supplied in the power grid, and their priorities are also different. These priorities are determined by electricity companies. Several factors such as of load importance, load location, and social criteria may be considered to determine these priorities. In the proposed algorithm, these priorities are assumed as input parameters and they are deterministic parameters for the algorithm. For instance, the importance of supplying energy to a hospital is obviously higher than residential customers. Therefore, the priority factor for hospital is higher than residential customers. As the priority of the loads in a distribution system is different, the power price for every load will also be different. DRP is an economical, reliable, and resilient method for enhancing the resilience of the distribution network. Some loads may have a DR contract, while others may not. Only loads that have DR contracts can participate in DRP. There are different types for DRP. In this research,

**Fig. 3** Proposed framework

the dynamic pricing model is used as the DRP. Dynamic pricing is a strategy used in demand response programs to manage and influence energy consumption based on real-time or forecasted changes in electricity prices. In this model, prices are adjusted in real-time based on current supply and demand conditions. The proposed DRP program has several steps. Electricity price depends on power consumption, and it increases step by step. Each step includes a specific percentage of the total load. The amounts of DR in different steps are not necessarily equal. The electricity price increases in each step; therefore, the first step has the lowest price. The proposed framework procedure is provided in Fig. 3.

## 4 Problem formulation

Multi-objective functions are introduced in this section to increase power grid resilience under wildfire. In this research, based on [10], resiliency is defined as the flexible ability of an electricity grid to restore itself and operate reliably in the event of any outages or blackouts. Power grid flexibility illustrates the level of system resourcefulness which enables a faster recovery process. It depends on the component's connectivity and its level of dependency on other elements. This index is defined as the ratio of the system's level of performance to that in the system's normal conditions.

$$f1 : \max \left( \frac{\sum_{i=1}^L (1 - y_{s,i}) P_i^L}{\sum_{i=1}^L P_i^B} \right) \quad (4)$$

The second objective function is to maximize the weighted restored loads while minimizing the responsive loads, which can be given as follows:

$$f2 : \max \left( \sum_{i \in L} (1 - y_{s,i}) \Gamma_i w_i \right)$$

$$- \sum_{i \in \Psi} \sum_{d \in \Upsilon} ((1 - y_{s,i}) \Gamma_i \Phi_i c_{id}) \quad (5)$$

where  $y_{s,i}$  indicates the probability of fire spreading to the area corresponding to  $i$ th bus.

The third objective function is to maximize capacity accessibility. Capacity adequacy is a vital factor that is playing a critical role in system resilience. Higher capacity adequacy during the wildfire leads to higher accessibility to the capacity. The resilience of the power grid can be obtained by maximizing the following equation:

$$f3 : \max \left\{ \frac{\sum_{i=t_0}^{t_1} \sum_{\ell=1}^L y_{s,\ell} (p_{bat\_dis,\ell,i} + p_{bat\_cha,\ell,i} + P_{G,i,\ell})}{\left( \sum_{q \in Q} (R_{q-\ell} \times \bar{P}_q) \right) T_e + \sum_{q \in Q} \bar{P}_q} \right\}$$

$$\frac{\sum_{i=t_0}^{t_1} \sum_{b=1}^L \left( S_{\ell,b} \times \left( \sum_{q \in Q} (R_{q-\ell} \times \bar{P}_q) \right) \right)}{T \sum_{q \in Q} \bar{P}_q} \quad (6)$$

where  $R_{q-\ell}$  is reachability between node  $q$  and  $\ell$  and is defined as the probability that node  $q$  and  $\ell$  are within the same island. In the complex power grids, this probability can be calculated using Monte Carlo simulation. A method in [23] estimates the energy remaining in the batteries based on the air temperature. This method used a neural network to calculate the energy that remained in the batteries. Although, other methods such as method [24] can be used to estimate parameters of the battery.

Constraints of the proposed algorithm for radial distribution networks are as follows:

$$\sum_{t \in B_i} (P_{it}) - \sum_{j \in A_i} (P_{ji} - R_{ji} I_{ji}^2) = P_i^{In}, \quad \forall i \in N \quad (7)$$

$$\sum_{t \in B_i} (Q_{it}) - \sum_{j \in A_i} (Q_{ji} - X_{ji} I_{ji}^2) = Q_i^{In}, \quad \forall i \in N \quad (8)$$

$$P_i^{In} = P_i^G - P_i^L, \quad \forall i \in N \quad (9)$$

$$Q_i^{In} = Q_i^G - Q_i^L, \quad \forall i \in N \quad (10)$$

$$I_{ij}^2 = \frac{P_{ij}^2 + Q_{ij}^2}{V_i^2}, \quad \forall (i, j) \in E \quad (11)$$

$$\xi_{ij} P_{ij}^{\min} \leq P_{ij} \leq \xi_{ij} P_{ij}^{\max}, \quad \forall (i, j) \in E \quad (12)$$

$$\xi_{ij} Q_{ij}^{\min} \leq Q_{ij} \leq \xi_{ij} Q_{ij}^{\max}, \quad \forall (i, j) \in E \quad (13)$$

$$V_i^2 - V_j^2 - 2(R_{ij} P_{ij} + X_{ij} Q_{ij}) + (R_{ij}^2 + X_{ij}^2) I_{ij}^2 = 0, \quad \forall (i, j) \in E \quad (14)$$

$$V_i^{\min} \leq V_i \leq V_i^{\max}, \quad \forall i \in N \quad (15)$$

$$0 \leq I_{ij} \leq I_{ij}^{\max}, \quad \forall (i, j) \in E \quad (16)$$

$$P_i^{DG, \min} \leq P_i \leq P_i^{DG, \max}, \quad \forall i \in G \quad (17)$$

$$Q_i^{DG, \min} \leq Q_i \leq Q_i^{DG, \max}, \quad \forall i \in G \quad (18)$$

$$0 \leq p_{bat\_dis, \ell, i} \leq \psi_{bat\_dis, b, \ell} \times B_{bat}^{\ell}, \quad i = t_0, \dots, t_1; \quad \ell = 1, \dots, L; \quad (19)$$

$$0 \leq p_{bat\_cha, \ell, i} \leq \psi_{bat\_cha, \ell, i} \times B_{bat}^{\ell}, \quad i = t_0, \dots, t_1; \quad \ell = 1, \dots, L; \quad (20)$$

$$\psi_{bat\_dis, \ell, i} + \psi_{bat\_cha, \ell, i} \leq 1, \quad i = t_0, \dots, t_1; \quad \ell = 1, \dots, L; \quad (21)$$

$$\psi_{bat\_dis, \ell, i}, \psi_{bat\_cha, \ell, i} \in \{0, 1\}, \quad i = t_0, \dots, t_1; \quad \ell = 1, \dots, L; \quad (22)$$

$$p_{bat\_dis, \ell, i} - p_{bat\_cha, \ell, i} + R_{ubat, \ell, i} \leq B_{bat}^{\ell}, \quad \ell = 1, \dots, L; \quad i = t_0, \dots, t_1; \quad (23)$$

$$p_{bat\_dis, \ell, i} - p_{bat\_cha, \ell, i} - R_{dbat, \ell, i} \geq -B_{bat}^{\ell}, \quad \ell = 1, \dots, L; \quad i = t_0, \dots, t_1; \quad (24)$$

$$0 \leq R_{ubat, \ell, i} \leq B_{bat}^{\ell}, \quad \ell = 1, \dots, L; \quad i = t_0, \dots, t_1; \quad (24)$$

$$0 \leq R_{dbat, \ell, i} \leq B_{bat}^{\ell}, \quad \ell = 1, \dots, L; \quad i = t_0, \dots, t_1; \quad (25)$$

$$S_{\ell, i} - S_{\ell, i-1} = \frac{p_{bat\_dis, \ell, i}}{\eta^+ - \eta^- (p_{bat\_dis, \ell, i})}, \quad \ell = 1, \dots, L; \quad i = t_0, \dots, t_1; \quad (26)$$

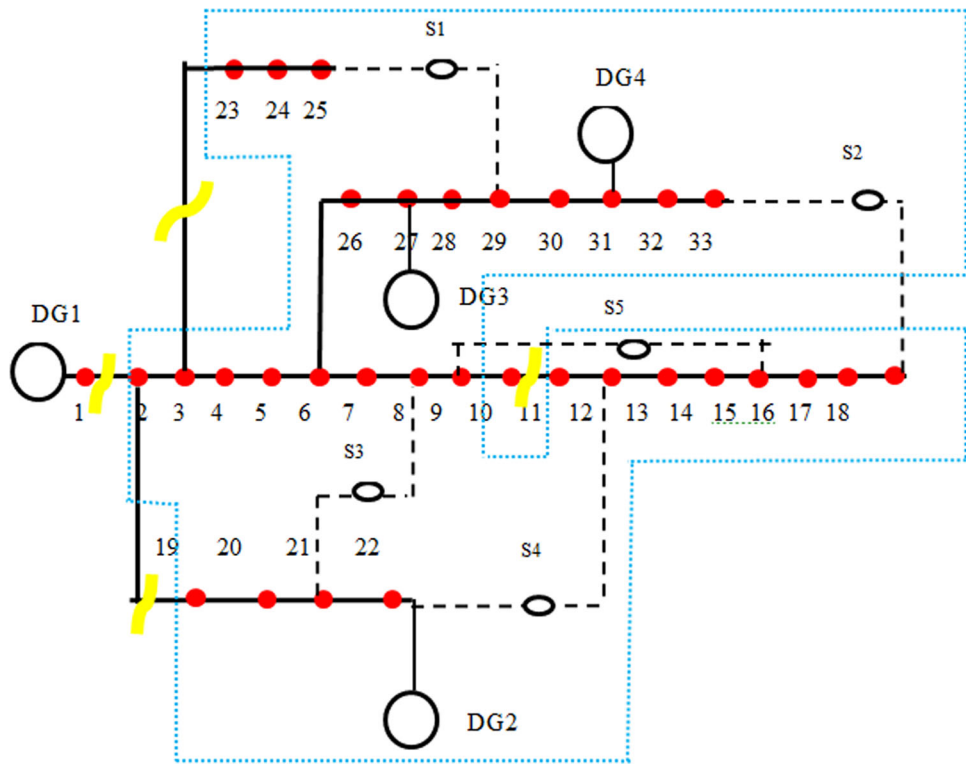
$$S_{\ell, t=t_1} \geq S_i^0 B_{bat-en}^{\ell}, \quad \ell = 1, \dots, L; \quad (27)$$

$$S_{\ell}^{\min} \times B_{bat-en}^{\ell} \leq S_{\ell, i} \leq S_{\ell}^{\max} \times B_{bat-en}^{\ell}, \quad \ell = 1, \dots, L; \quad i = t_0, \dots, t_1; \quad (28)$$

In the proposed model, both active and reactive power are considered. Equations (7) and (8) represent active and reactive line flows, respectively. Constraints in (9) and (10) show nodal active and reactive power flows, respectively. The magnitude of current for each line is obtained from (11). Equations (12) and (13) show the maximum active and reactive power that are transmitted through transmission lines, respectively. Variable  $\xi$  is a binary variable which indicates switch states in transmission lines. For lines that do not have a switch, this value is considered equal to one. Equation (14) provides the Ohm law over each line. The bus voltage magnitude and line currents are limited by Constraints (15) and (16), respectively. Constraints in (17) and (18) limit the generated active and reactive power by each DG, respectively. It is assumed that some DGs such as photovoltaic do not produce reactive power. Constraints (19) and (20) indicate that the generated power by battery power is less than the maximum power capacity. Constraints (21) and (22) guarantee battery only can charge or discharge at each time. Equations (23) and (24) set the charging/discharging power of the battery storage based on its ramp service within its charging/discharging limits. Equations (25) and (26) regulate the battery ramp service based on its capacity limits. Eqs. (27), (28), and (29) indicate that the energy remaining in the battery is restricted by battery charging and discharging efficiency. It is observed, in mathematical definition of the proposed problem, KVL and KCL rules are considered in definition of problem constraints, buses are considered as node, and the power grid can be modeled as graph. Constraints in (7), (8), (9), (10), (11), and (14) provide opportunity to include other fundamental components, such as transformers and substations. Therefore, the proposed model can be sufficient to fully capture the impact of wildfires on the power grid.

In the proposed framework, it is assumed that some loads have DR contracts and participate in DRP. After a critical load restoration program, loads without DR contracts can be restored or not. Variable  $w_i$  is binary. The zero state means that the  $i$ th load will turn off after the critical load restoration program, while the one state means, it will be restored. Loads with DR contract may be restored partially. Therefore, active

**Fig. 4** The topology of distribution system after a wildfire



and reactive power for the  $i$ th load can be obtained as follows:

$$P_i^L = \begin{cases} P_i^B, & \text{if } i^{\text{th}} \text{ load has high priority} \\ P_i^D, & \text{if } i^{\text{th}} \text{ load has DR contract} \\ w_i P_i^B, & \text{if } i^{\text{th}} \text{ load does not have DR contract} \end{cases} \quad (30)$$

$$Q_i^L = \begin{cases} P_i^B \times \tan(\phi_i), & \text{if } i^{\text{th}} \text{ load has high priority} \\ P_i^D \times \tan(\phi_i), & \text{if } i^{\text{th}} \text{ load has DR contract} \\ w_i P_i^B \times \tan(\phi_i), & \text{if } i^{\text{th}} \text{ load does not have DR contract} \end{cases} \quad (31)$$

where  $\phi$  is the power angle and:

As demonstrated in Fig. 1, DRP is defined in  $d$  steps. The capacity of each step is shown by  $P_{id}^{\text{StepDR}}$ . The electricity price is increased in each step. When the  $i$ th load utilizes DRP in step  $k$ , it means that its power consumption has been more than the sum of previous steps ( $k-1$  steps). In this case, it is possible to use only part of the capacity in the  $k$ th step as shown in:

$$P_i^D \leq \sum_{d \in \Upsilon} (P_{id}^{\text{StepDR}} \cdot c_{id}), \quad \forall i \in \Psi \quad (32)$$

## 5 Case studies

In this study, the performance of the proposed algorithm is investigated using the modified 33-bus system [25]. This research utilizes the multi-objective particle swarm optimization (PSO) algorithm due to its numerous advantages. These advantages include simple implementation, a small number of parameters to be tuned, the ability to run parallel computations, robustness, higher efficiency and probability

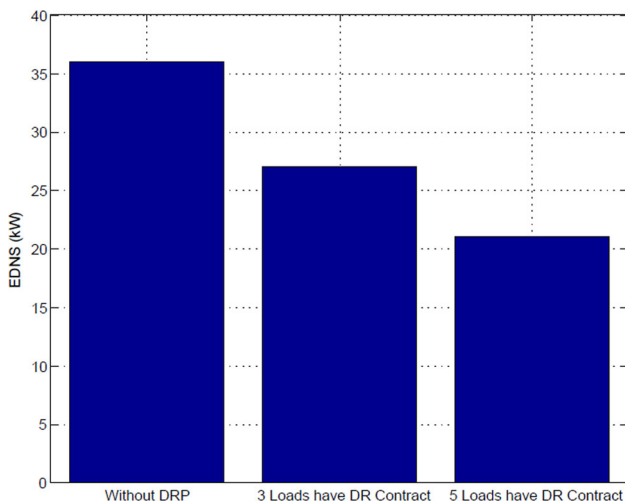
of finding the global optima, low computational time, and more. PSO algorithm is developed based on levy flight and double-archive mechanism and was introduced in [26]. In this algorithm, levy flight is combined with PSO to avoid the algorithm falling into local optima. Using modified PSO algorithm, more useful particles can be kept, and thus, the diversity of the solutions is increased. This algorithm has fast convergence and higher accuracy than other state-of-the-art multi-objective heuristic algorithms. Also, performance of PSO algorithm is compared with genetic algorithm (GA) and firefly algorithm.

**Table 2** DGs data

Generator	Bus	Type	Qmax (kVAR)	Pmax (kW)
DG1	1	Thermal	300	500
DG2	22	Thermal	100	350
DG3	27	Thermal	200	400
DG4	31	Photovoltaic	—	200

**Table 3** Priorities of loads

Node number	Priority	Priority factor
4, 8, 14, 21	High	10
5, 12, 17, 24, 29	Medium	1
Other nodes	Low	0.1

**Fig. 5** EDNS for distribution system for PSO algorithm

This system is shown in Fig. 4. There are four DGs in the system. Parameters of these DGs are provided in Table 2. It is assumed that DGs 1–3 are thermal plants and DG4 is a solar plant with photovoltaic cells. In the distribution system, the priorities of loads are different. The solar power plant does not generate reactive power and is connected to the grid via an inverter. It is assumed that loads have three priorities, which are presented in Table 3. The priority factor for a high-priority load is assumed to be 10, and for medium- and low-priority loads, its values are 1 and 0.1, respectively. High-priority loads do not participate in DRP. In this study, it is assumed that only low-priority loads participate in DRP. The DRP model has four steps in which the energy cost increases step by step.

A wildfire may cut some transmission lines. The yellow dashed lines shown in Fig. 5 indicate damaged lines. The capacity of the remaining lines will also be reduced due to their distance from the wildfire. DGs and transmission lines

**Table 4** The performance of distribution system after a wildfire

Three loads have DRP contract			Five loads have DRP contract		
Bus	Load (kW)	DR steps	Bus	Load (kW)	DR steps
6	60	(1,1,0,0)	6	60	(1,1,0,0)
15	60	(1,1,1,0)	15	60	(1,1,0,0)
20	80	(1,1,1,1)	20	80	(1,1,1,0)
			23	100	(1,1,1,1)
			30	70	(1,1,0,0)

near to the wildfire tolerate more heat. As a result, their capacity is further reduced. For example, in Fig. 5, the impact of fire on DG4 is less than that of DG1, and the transmission line between nodes 17 and 18 is less affected by fire than the transmission line between nodes 11 and 12. After wildfire, the optimal states of switches and the optimal system parameters are calculated using the proposed algorithm. Therefore, the switches and tie lines will be closed, and the grid configuration will be changed. In this figure, it can be seen that all nodes, except node 1, are energized after changing the grid configuration. The blue-dotted lines demonstrate that all nodes in the network are still energized, and the distribution system has shown resilience against wildfire.

As shown in Table 3, priorities of loads are different. Proposed algorithm attempts to restore high-priority loads. Moreover, only some loads have DR contract and participate in DRP. Electricity price for these loads is changed in several steps. In this case, the algorithm can only turn ON or OFF the loads that do not have a DR contract.

System performance is evaluated in three scenarios. In the first scenario, it is assumed that none of the loads have the DRP contract. In the other scenarios, it is presumed that some loads have the DRP contract. The details of these three scenarios are given in Table 4. This table shows that some loads have used two DRP steps, while others have employed more steps. The results for PSO algorithm are presented in Figs. 5 and 6. EDNS metric indicates the power demand that is not supplied. Using DRP, the power demand is managed. Therefore, the amount of EDNS is reduced. If more loads participate in the DRP, the amount of EDNS will be further reduced. Low-priority loads that do not have a DR contract

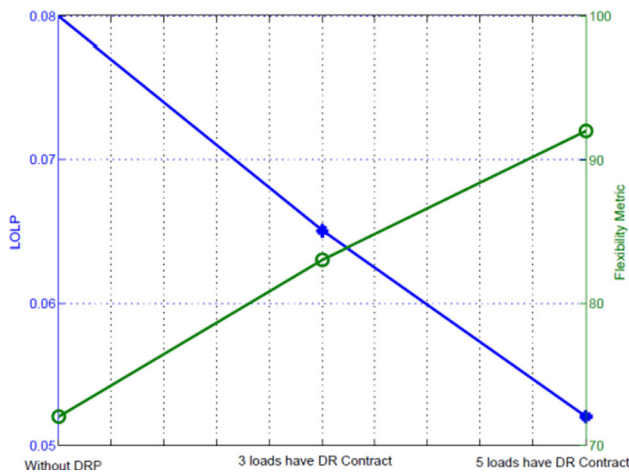


**Fig. 6** LOLP and flexibility metrics for distribution system for PSO algorithm

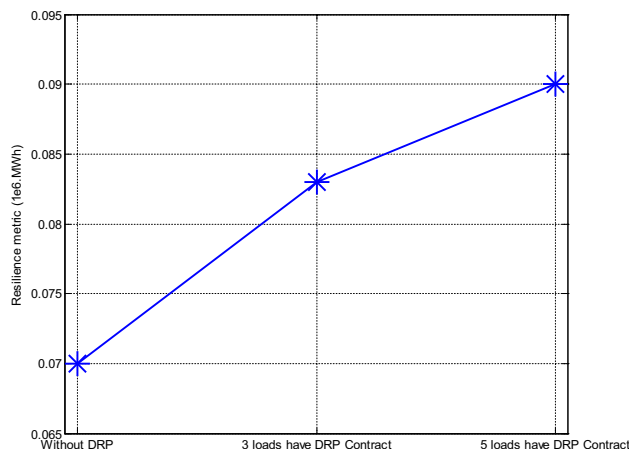


**Fig. 7** Resilience metric for different DRP scenarios for PSO algorithm

may be turn OFF. In the first scenario, the number of OFF loads was equal to 5, while in the second and third scenarios, this number reduced to 4 and 2, respectively. For the first scenario, the minimum voltage of the system is 0.9636 per unit while for second and third scenarios are 0.9772 and 0.9876 per unit, respectively. Also, power losses for all three scenarios are 135.46, 98.29, and 79.47 kW, respectively. Figure 6 shows the LOLP and flexibility metrics for different assumptions. Flexibility metric is shown in percent. It is observed that the value of LOLP decreases by raising the number of loads that have DR contracts. Figure. 7 shows resilience metric for different scenarios when the PSO algorithm is used as optimization algorithm. In this figure, capacity accessibility is used as resilience metric. It can be seen that with the increase in the number of subscribers who participate in DRP, the amount of capacity accessibility also increases. These figures display that the DRP contract can improve system

**Table 5** Compare performance of algorithms

Scenario		without DRP	Three loads have DRP	Five loads have DRP
LOLP	PSO	0.08	0.065	0.052
	Firefly	0.083	0.066	0.055
	GA	0.086	0.068	0.056
EDNS (Kw)	PSO	36.24	27.71	22.42
	Firefly	38.71	28.56	24.06
	GA	39.09	29.77	24.83
Flexibility metric (%)	PSO	72	84	93
	Firefly	70	82	90
	GA	69	79	88
Resilience metric ( $10^6$ MWh)	PSO	0.07	0.0825	0.09
	Firefly	0.065	0.073	0.085
	GA	0.066	0.071	0.083
Minimum voltage (pu)	PSO	0.9636	0.9772	0.9876
	Firefly	0.9621	0.9712	0.9811
	GA	0.9579	0.9691	0.9801
Power losses (Kw)	PSO	135.46	98.29	79.47
	Firefly	134.41	103.91	87.65
	GA	132.16	105.44	91.08

performance and thus its resilience against wildfire. Moreover, the simulation results show that the proposed algorithm is able to provide the energy required for high-priority loads in all three scenarios. Table 5 compares the performance of PSO with GA and firefly algorithms. In this table, the flexibility metric is shown in percent. It is observed, for the proposed problem. The performance of the modified PSO algorithm is better than GA and firefly algorithms. Also, this table shows that the firefly algorithm has a better performance than the GA.

Now, suppose that the wildfire has spread from different areas, and the transmission lines between Nodes 7 and 8, and Nodes 16 and 17 are out of service. In this case, more transmission lines are affected by the heat of the wildfire and the damage to the network will be greater. The proposed algorithm determines both the optimal system topology and the optimal system parameters. System topology is shown in Fig. 8. It is observed in this scenario that the distribution network is divided into two separate sub-grids while there is no connection between them. In this figure, the sub-grids are marked with blue- and green-dotted lines. As observed, MICROGRID1 has only one DG while MICROGRID2 has two DGs, one of which is photovoltaic.

Again, network performance is investigated in three scenarios, and network resilience is assessed by the EDNS metric. The results for PSO algorithm are presented in Fig. 9.

**Fig. 8** The topology of distribution system after a wildfire

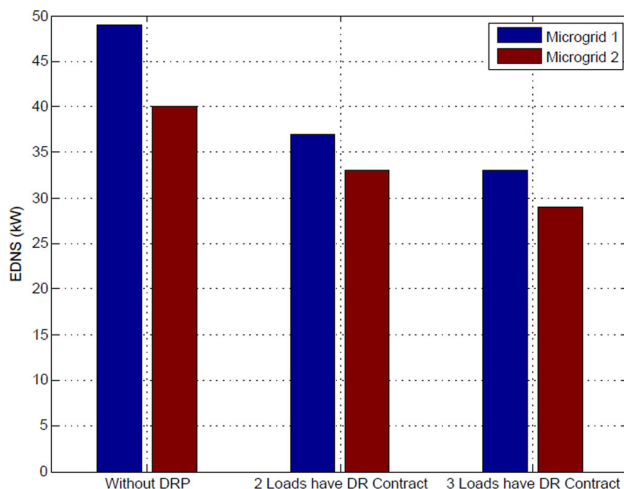
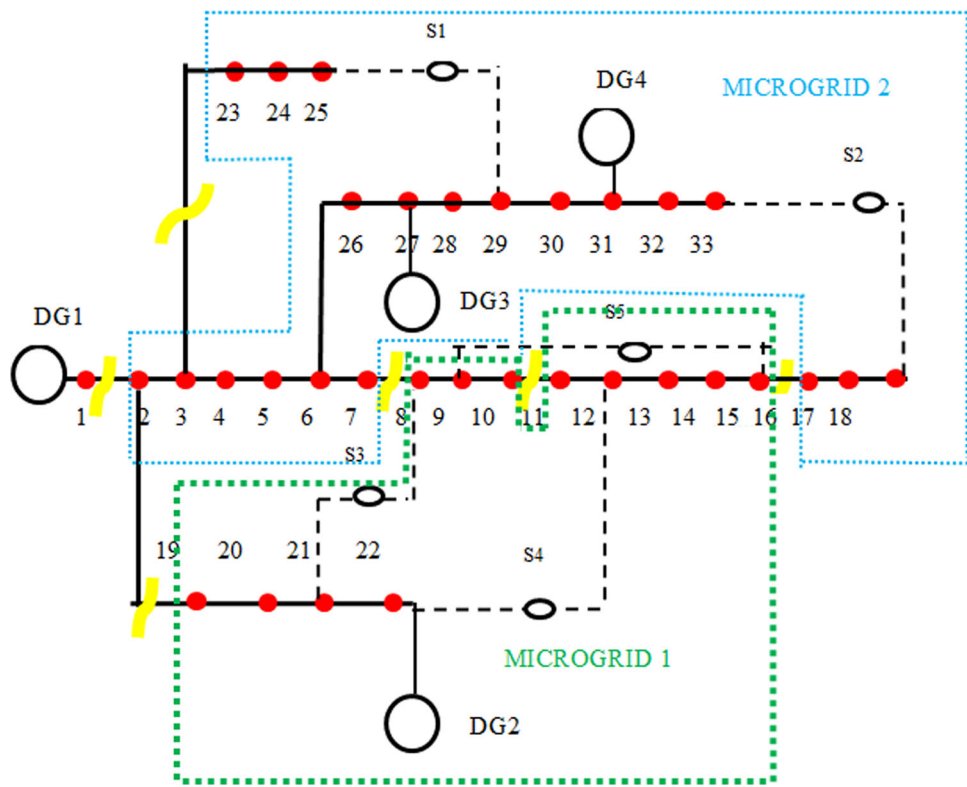


**Fig. 9** EDNS for distribution systems for PSO algorithm

This figure shows that the DRP program reduces the EDNS. The values of EDNS for the MICROGRID1 are higher than MICROGRID2, because, there are two power plants in MICROGRID2, including a solar power plant and a thermal power plant. In addition, buses in MICROGRID2 are further away from fire sites. The values of LOLP and flexibility system metrics for PSO algorithm are shown in Fig. 10. As seen, the increase in wildfire causes the network resilience to decline. Moreover, this figure indicates that the performance of the power grid is improved by using the DR program.

When PSO algorithm is used, the obtained value for capacity accessibility metric in both microgrids is shown in Fig. 11. It is observed that the resilience of the second microgrid is more than the first microgrid, and in both microgrids, with the increase in the number of subscribers who have participated in DRP, the resilience is also improved. Table 6 indicates results of PSO, GA, and firefly algorithms. Similar to PSO, GA and firefly algorithms divide power grid into two microgrids. For this example, due to location of damaged lines and small size of power grid, topology of grid after optimization is similar for all optimization algorithms. In other words, results for states of tie switches are same for all algorithms. For complicated power grids with a lot of tie lines, topology of power grid after wildfire may be different for different algorithms. This table indicates the PSO algorithm has the best performance, while the performance of firefly algorithm is better than GA and worse than PSO.

The simulation results indicate that the distribution system is not able to provide the energy required for all loads. In the first scenario, the proposed algorithm does not guarantee the power supply for all high-priority loads. However, in second and third scenario, the proposed algorithm provides power for all high-priority loads. In both sub-grids, for all scenarios, some low-priority loads are disconnected from the network.

**Fig. 10** LOLP and flexibility metrics for distribution systems for PSO algorithm

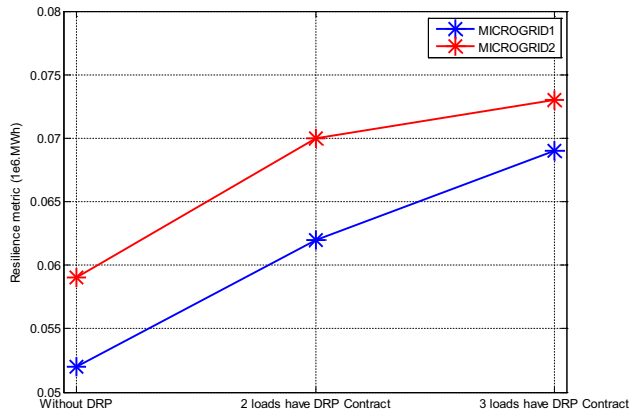
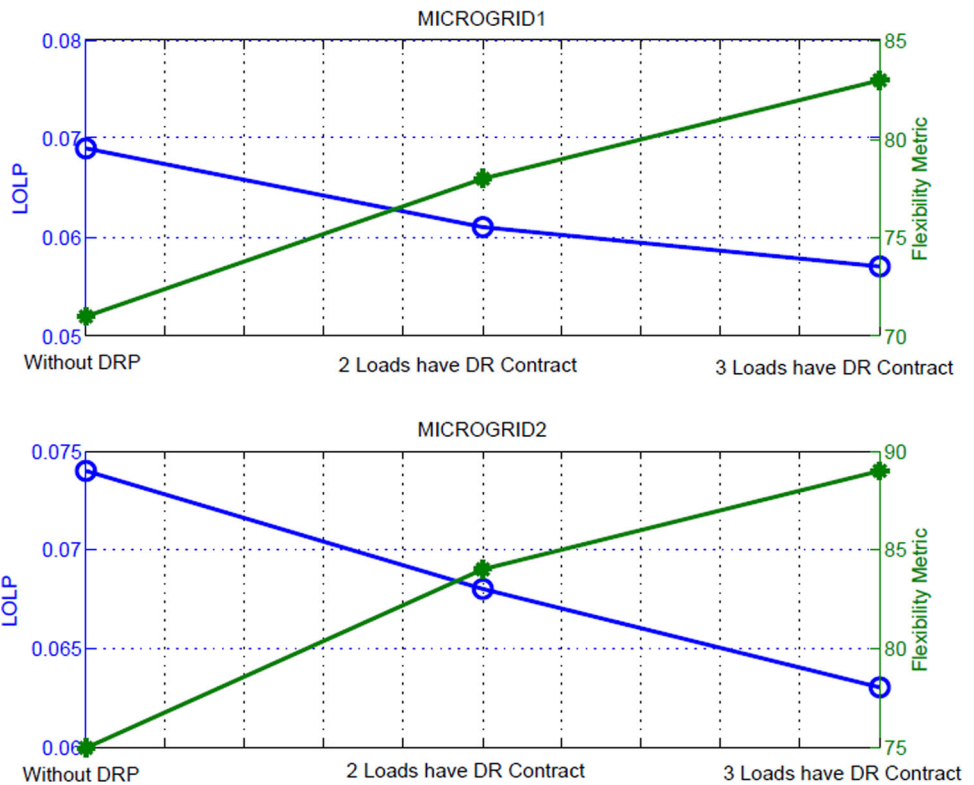


**Fig. 11** Resilience metric for different DRP scenarios for PSO algorithm

In addition, loads with DRP contract pay more price than the previous scenario.

## 6 Conclusion

A framework for the optimal reconfiguration of a power grid after a wildfire and energy supply for high-priority loads has

been introduced in this paper. A novel multi-objective problem has been presented to optimize power grid flexibility and maximize the weighted restored loads while minimizing the responsive loads. The probability of fire spreading to each area has also been considered in the framework. The optimization algorithm is able to manage the power consumption in loads that have DR contracts and interrupt the power flow for other low-priority loads. This proposed model calculates the optimal variables of the power grid during a wildfire. The performance of the proposed algorithm has been investigated by applying it on the 33-bus test systems. The resilience of the power grid has been assessed by LOLP, EDNS, and power grid flexibility metrics. The simulation results indicate that the proposed algorithm successfully calculates the optimal topology of the grid after a wildfire, while the DR program can improve power grid resilience. In future work, optimal scheduling for charging and discharging of storage device will be investigated and the proposed framework will be improved by adding a new objective function for this purpose.

**Table 6** Compare performance of algorithms

Scenario		Without DRP		Three loads have DRP		Five loads have DRP	
Topology		Microgrid 1	Microgrid 2	Microgrid 1	Microgrid 2	Microgrid 1	Microgrid 2
LOLP	PSO	0.068	0.074	0.061	0.068	0.058	0.063
	Firefly	0.071	0.076	0.063	0.069	0.061	0.065
	GA	0.072	0.077	0.064	0.071	0.062	0.065
EDNS (Kw)	PSO	49.42	40.03	37.76	33.76	34.21	28.82
	Firefly	53.24	42.09	39.25	34.46	36.17	29.74
	GA	54.66	43.29	40.08	36.82	37.24	30.98
Flexibility metric (%)	PSO	72	75	77	84	83	88
	Firefly	69	74	76	82	79	84
	GA	68	72	75	81	79	83
Resilience metric (106 MWh)	PSO	0.053	0.058	0.063	0.07	0.069	0.073
	Firefly	0.051	0.055	0.06	0.067	0.065	0.07
	GA	0.049	0.054	0.06	0.065	0.062	0.067
Minimum voltage (pu)	PSO	0.9611	0.9633	0.9694	0.9712	0.9723	0.9796
	Firefly	0.9601	0.9622	0.9682	0.9689	0.9714	0.9867
	GA	0.9514	0.9616	0.9671	0.9685	0.9705	0.9748
Power losses (Kw)	PSO	68.33	57.19	59.48	49.57	56.24	46.77
	Firefly	71.26	59.63	62.21	53.13	59.66	48.75
	GA	72.51	60.09	62.97	55.16	61.11	49.64

**Author contribution** S. Najibi conceived of the presented idea. S. Najibi and M. Najafi developed the theory and performed the computations. S. Najibi and M. Najafi verified the analytical methods. M. Najafi and M. Mallaki and N. Cheraghi to investigate [a specific aspect] and supervised the findings of this work. All authors discussed the results and contributed to the final manuscript.

## Declarations

**Conflict of interest** The author declare that they have no conflict of interest.

## References

- Sayarshad HR (2023) Preignition risk mitigation model for analysis of wildfires caused by electrical power conductors. *Int J Elect Power Energy Syst.* <https://doi.org/10.1016/j.ijepes.2023.109353>
- Nazaripoura H (2020) Power grid resilience under wildfire: a review on challenges and solutions. *ieee power & energy society general meeting (PESGM)*, Montreal, QC, Canada. <https://doi.org/10.1109/PESGM41954.2020.9281708>
- Mitchell JW (2023) Analysis of utility wildfire risk assessments and mitigations in California. *Fire Saf J.* <https://doi.org/10.1016/jfiresaf.2023.103879>
- Sarkar M, Yan X, Erol BA, Raptis I, Homaifar A (2021) A novel search and survey technique for unmanned aerial systems in detecting and estimating the area for wildfires. *Robot Auton Syst.* <https://doi.org/10.1016/j.robot.2021.103848>
- Najibi S, Najafi M, Mallaki M, Cheraghi Shirazi N (2022) Corrigendum to “smart grid resiliency improvement using a multi-objective optimization approach” [Sustain. Energy Grids Netw. 32, 2022 100886]. *Sustain Energy, Grids Netw.* <https://doi.org/10.1016/j.segan.2022.100886>
- Yang W, Sparrow SN, Ashtine M, Wallom DCH, Morstyn T (2022) Resilient by design: preventing wildfires and blackouts with microgrids. *Appl Energy.* <https://doi.org/10.1016/j.apenergy.2022.118793>
- Panteli M, Mancarella P (2015) Influence of extreme weather and climate change on the resilience of power systems: impacts and possible mitigation strategies. *Electr Power Syst Res* 127:259–270. <https://doi.org/10.1016/j.epsr.2015.06.012>
- Ansari B, Mohagheghi S (2014) Optimal energy dispatch of the power distribution network during the course of a progressing wildfire. *Int Trans Electr Energy Syst* 25:3422–3428. <https://doi.org/10.1002/etep.2043>
- Kahnamouei A S, Lotfifard S (2021) Enhancing Resilience of Distribution Networks by Coordinating Microgrids and Demand Response Programs in Service Restoration. *arXiv*, 2021. [Online]. Available: <https://arxiv.org/abs/2107.06347>.
- Perera ATD, Zhao B, Wang Z, Soga K, Hong T (2023) Optimal design of microgrids to improve wildfire resilience for vulnerable communities at the wildland-urban interface. *Appl Energy.* <https://doi.org/10.1016/j.apenergy.2023.120744>
- Abdelmalak M, Benidris M (2022) Enhancing power system operational resilience against wildfires. *IEEE Trans Ind Appl* 58:1611–1621. <https://doi.org/10.1109/TIA.2022.3145765>
- Salimi AH, Nazaripoura H (2023) Equitable operational resilience of power distribution grids in the face of progressive wildfires. *North Am Power Symp (NAPS)*. <https://doi.org/10.1109/NAPS58826.2023.10318605>
- Dehghanian P, Nazemi M (2023) Powering through wildfires: an integrated solution for enhanced safety and resilience in power grids. *IEEE Trans Ind Appl* 53:4192–4202. <https://doi.org/10.1109/TIA.2022.3160421>

14. Parsibenehkhal R, Jamil M, Khan AA (2024) A multi-stage framework for coordinated scheduling of networked microgrids in active distribution systems with hydrogen refueling and charging stations. *Int J Hydrogen Energy* 71:1442–1455. <https://doi.org/10.1016/j.ijhydene.2024.05.364>
15. Zhang H, Ma Y, Yuan K, Khayatnezhad M, Ghadimi N (2024) Efficient design of energy microgrid management system: a promoted Remora optimization algorithm-based approach. *Heliyon*. <https://doi.org/10.1016/j.heliyon.2023.e23394>
16. Ghadimi N, Yasoubi E, Akbari E, Sabzalian MH (2023) SqueezeNet for the forecasting of the energy demand using a combined version of the sewing training-based optimization algorithm. *Heliyon*. <https://doi.org/10.1016/j.heliyon.2023.e16827>
17. Chang L, Wu Z, Ghadimi N (2023) A new biomass-based hybrid energy system integrated with a flue gas condensation process and energy storage option: an effort to mitigate environmental hazards. *Process Saf Environ Prot* 177:959–975. <https://doi.org/10.1016/j.psep.2023.07.045>
18. Najibi S, Najafi M, Mallaki M, Shirazi NC (2022) Power demand estimation during pandemic times: the case of the COVID-19 in Tehran Iran. *J Manag Technol* 6:176–187. <https://doi.org/10.22109/JEMT.2021.278673.1289>
19. Choobineh M, Ansari B, Mohagheghi S (2015) Vulnerability assessment of the power grid against progressing wildfires. *Fire Safety J* 73:20–28. <https://doi.org/10.1109/TPWRS.2012.2184307>
20. Subramanian V, Das TK (2019) A two-layer model for dynamic pricing of electricity and optimal charging of electric vehicles under price spikes. *Energy* 167:1266–1277. <https://doi.org/10.1016/j.energy.2018.10.171>
21. Abdin IF, Fang Y, Zio E (2019) A modeling and optimization framework for power systems design with operational flexibility and resilience against extreme heat waves and drought events. *Renew Sustain Energy Rev* 112:706–719. <https://doi.org/10.1016/j.rser.2019.06.006>
22. Gilletly SD, Jackson ND, Staid A (2023) Evaluating the impact of wildfire smoke on solar photovoltaic production. *Appl Energy*. <https://doi.org/10.1016/j.apenergy.2023.121303>
23. Mallaki M, Najibi S, Najafi M, Shirazi NC (2022) Smart grid resiliency improvement using a multi-objective optimization approach. *J Sust Energy, Grids Netw*. <https://doi.org/10.1016/j.sgan.2022.100886>
24. Yuan K, Ma Y, Zhang H, Razmjoo N, Ghadimi N (2023) Optimal parameters estimation of the proton exchange membrane fuel cell stacks using a combined owl search algorithm. *Heliyon*. <https://doi.org/10.1080/15567036.2023.2252672>
25. Li X, Li B, Li F, Zhang R, Chen H (2022) Modified IEEE 33-bus and 123-bus ac-dc hybrid test systems. *IEEE Data part*. <https://doi.org/10.21227/fcsp-f683>
26. Guan T, Han F, Han H (2019) A modified multi-objective particle swarm optimization based on levy flight and double-archive mechanism. *IEEE Access* 7:183444–183467. <https://doi.org/10.1109/ACCESS.2019.2960472>

**Publisher's Note** Springer Nature remains neutral with regard to jurisdictional claims in published maps and institutional affiliations.

Springer Nature or its licensor (e.g. a society or other partner) holds exclusive rights to this article under a publishing agreement with the author(s) or other rightsholder(s); author self-archiving of the accepted manuscript version of this article is solely governed by the terms of such publishing agreement and applicable law.

## Terms and Conditions

Springer Nature journal content, brought to you courtesy of Springer Nature Customer Service Center GmbH (“Springer Nature”). Springer Nature supports a reasonable amount of sharing of research papers by authors, subscribers and authorised users (“Users”), for small-scale personal, non-commercial use provided that all copyright, trade and service marks and other proprietary notices are maintained. By accessing, sharing, receiving or otherwise using the Springer Nature journal content you agree to these terms of use (“Terms”). For these purposes, Springer Nature considers academic use (by researchers and students) to be non-commercial.

These Terms are supplementary and will apply in addition to any applicable website terms and conditions, a relevant site licence or a personal subscription. These Terms will prevail over any conflict or ambiguity with regards to the relevant terms, a site licence or a personal subscription (to the extent of the conflict or ambiguity only). For Creative Commons-licensed articles, the terms of the Creative Commons license used will apply.

We collect and use personal data to provide access to the Springer Nature journal content. We may also use these personal data internally within ResearchGate and Springer Nature and as agreed share it, in an anonymised way, for purposes of tracking, analysis and reporting. We will not otherwise disclose your personal data outside the ResearchGate or the Springer Nature group of companies unless we have your permission as detailed in the Privacy Policy.

While Users may use the Springer Nature journal content for small scale, personal non-commercial use, it is important to note that Users may not:

1. use such content for the purpose of providing other users with access on a regular or large scale basis or as a means to circumvent access control;
2. use such content where to do so would be considered a criminal or statutory offence in any jurisdiction, or gives rise to civil liability, or is otherwise unlawful;
3. falsely or misleadingly imply or suggest endorsement, approval , sponsorship, or association unless explicitly agreed to by Springer Nature in writing;
4. use bots or other automated methods to access the content or redirect messages
5. override any security feature or exclusionary protocol; or
6. share the content in order to create substitute for Springer Nature products or services or a systematic database of Springer Nature journal content.

In line with the restriction against commercial use, Springer Nature does not permit the creation of a product or service that creates revenue, royalties, rent or income from our content or its inclusion as part of a paid for service or for other commercial gain. Springer Nature journal content cannot be used for inter-library loans and librarians may not upload Springer Nature journal content on a large scale into their, or any other, institutional repository.

These terms of use are reviewed regularly and may be amended at any time. Springer Nature is not obligated to publish any information or content on this website and may remove it or features or functionality at our sole discretion, at any time with or without notice. Springer Nature may revoke this licence to you at any time and remove access to any copies of the Springer Nature journal content which have been saved.

To the fullest extent permitted by law, Springer Nature makes no warranties, representations or guarantees to Users, either express or implied with respect to the Springer nature journal content and all parties disclaim and waive any implied warranties or warranties imposed by law, including merchantability or fitness for any particular purpose.

Please note that these rights do not automatically extend to content, data or other material published by Springer Nature that may be licensed from third parties.

If you would like to use or distribute our Springer Nature journal content to a wider audience or on a regular basis or in any other manner not expressly permitted by these Terms, please contact Springer Nature at

[onlineservice@springernature.com](mailto:onlineservice@springernature.com)